RELATIVISTIC α-PARTICLES EMITTED
IN Fe-EMULSION INTERACTIONS AT 1.7A GeV

K.B. BHALLA, M. CHAUDHRY and S. LOKANATHAN

Department of Physics, University of Rajasthan, Jajpur, 302004 India

R.K. GROVER, I.K. DAFTARI, G.L. KAUL,
L.K. MAGOTRA, Y. PRAKASH and N.K. RAO

Department of Physics, University of Jammu, Jammu, 180001 India

and

S. GARPMAN and I. OTTERLUND

Department of Physics, University of Lund, S-223 62 Lund Sweden

Jajpur–Jammu–Lund collaboration

Abstract: Relativistic α-particles have been studied in 423 interactions of Fe in emulsion at 1.7A GeV. Comparisons of the observed angular distribution with that from ^{16}O-emulsion reactions at 2.1A GeV reveal that more α-particles are observed at large angles in the Fe-emulsion reactions. The α-particles at large angles cannot be explained by fragmentation from a clean-cut spectator. Comparison of the experimental data with moving relativistic Boltzmann distributions shows that a single Boltzmann distribution cannot fit the fragmentation peak and the tail simultaneously. A thermal source (fireball) explaining the tail part of the distribution needs to be formed by a mechanism other than a simple clean-cut participant-spectator process. A large transverse momentum transfer to the spectator before fragmentation may explain the tail.

1. Introduction

A study of relativistic α-particles can provide information about the fragmentation mechanism and thus help to trace the reaction mechanism of nucleus–nucleus interactions at high energies. Normally one would expect the relativistic α-particles to be emitted as a result of fragmentation of a projectile or a projectile spectator in the spectator-participant process. In this study it is shown that whereas the major fraction of these α-particles can be understood in terms of fragmentation of the projectile (or the projectile spectator), an appreciable fraction of α-particles observed at large angles must be produced by another mechanism. One possibility could be that they are emitted from a fireball in which the major component comes

from the projectile, having a velocity slightly less than that of the projectile and heated to a temperature in the range 30–60 MeV. This conclusion is drawn by comparing the experimentally measured angular distribution of relativistic α-particles with those calculated using moving relativistic Boltzmann distributions [1]).

Our calculations show that the α-particles scattered at large angles cannot be fitted unambiguously by moving Boltzmann distributions. Instead several combinations of the parameters (velocity β and temperature T of the source) minimize χ^2. To resolve the ambiguity we combined the previous information with that of the 4-momentum conservation of N_p and N_t, the numbers of participating nucleons from the projectile and the target, respectively (spectator-participant model). In this way unique values of the parameters β and T were obtained as the intercept of two curves in the β, T plane. However, the values obtained are not consistent with those from a clean-cut fireball model. A very peculiar fireball involving a small number of participating nucleons from the target and a large number from the projectile would result from the analysis of the tail part of the angular distribution. This is however, not an easily understandable picture of fireball formation. An alternative, but not very probable, explanation could be that the α-particle source is a fireball formed at high temperature and smaller velocity which subsequently cools by emission of light particles (pions, kaons, etc.) before the α-emission occurs. A more plausible explanation might be that the fragmenting nucleus gets a transverse momentum from the participating region before the emission of α-particles occurs. Such a transverse momentum would enhance the large-angle scattering. One might also imagine that hard scattering of pre-existing α-structures in the nuclear surfaces could explain this part of the angular distribution, at least partially.

2. Experimental results

The interactions of 423 Fe nuclei in emulsions at $1.7A$ GeV have been measured in the study of the emitted relativistic α-particles. These interactions form a random subsample chosen from a bigger collection of 1680 Fe interactions obtained by track scanning, the details of which are discussed elsewhere [2]). The relativistic α-particles at angles of up to 10° to the beam have been identified, and their angles, θ_α, measured. For the identification of α-particles, ionization measurements are made near the Fe interaction and also where α-tracks extend a distance of about 2 cm. If the ionization is about four times the minimum ionization and does not change in the second measurement the track is identified as due to a relativistic α-particle. Alternatively tracks having an ionization of four times g_{min}† or more could be due to grey tracks registered by slow singly charged particles i.e. p, d and t. However protons having an ionization of $4g_{min}$ would have a range ~2 cm, whereas the ionization would change to ~$5.5g_{min}$, if the tracks are due to deuterons.

---

† g_{min} is the plateau density of a singly charged particle.

The change in ionization in such tracks would be to $4.8g_{min}$ if they are due to tritons. The contribution from tritons can, however, be neglected because of two factors: firstly, the average number of grey tracks produced in the forward 10° cone is not large (~15%); secondly the probability that they are due to tritons is very small (≤10%). Whereas the contribution of $Z = 1$ particles is negligible, there may be a small percentage of tracks due to ^{3}He particles from the projectile.

Fig. 1b shows the measured angular distribution for the relativistic α-particles observed in all the 423 interactions. A comparison with the angular distribution of α-particles emitted in ^{16}O-emulsion [3]) reactions at 2.1A GeV is also presented. We see that for the Fe case the peak is broader and the tail becomes larger i.e. more α-particles exist at large angles in Fe reactions. For comparison of the angular distributions it will be convenient to define a tail to peak ratio as

$$R_{tp} = \frac{\text{number of } \alpha \text{ particles with } 10° \geqslant \theta_\alpha > 3°}{\text{number of } \alpha \text{ particles with } \theta_\alpha \leqslant 3°} . \tag{1}$$

We find that

$$R_{tp} = 0.383 \pm 0.029 \text{ for the Fe reaction,}$$

$$R_{tp} = 0.095 \pm 0.021 \text{ for } {}^{16}\text{O reactions .}$$

Comparison of ^{16}O data with a sample of 66 events with $N_h = 0$ (i.e. no observed slow target fragment) type events is presented in fig. 1a. The two distributions are quite similar i.e. $R_{tp} = 0.10$ for Fe reactions ($N_h = 0$ sample) and $R_{tp} = 0.095$ for ^{16}O reactions (general sample). It is important to stress here that there is no target fragmentation in the Fe events ($N_h = 0$, i.e. peripheral collisions), while in the ^{16}O reactions all impact parameters are represented. In spite of this the distributions are very similar and essentially given by the Fermi motion of the constituents in the nucleus. On the other hand when $N_h \geqslant 0$ the α-particles exhibit very different distributions in the ^{56}Fe and ^{16}O interactions.

Fig. 2 exhibits the comparison of angular distributions for the two cases: general sample (all N_h) and 66 events of $N_h = 0$ type. It can be seen that in the $N_h = 0$ sample, few α-particles are emitted with angles greater than expected from pure projectile fragmentation, whereas the proportion of these is much more pronounced in the general sample: $R_{tp} = 0.10$ for $N_h = 0$ events and $R_{tp} = 0.38$ for the general sample. The curve of $N_h = 0$ events and $R_{tp} = 0.38$ for the general sample. The curve of $N_h = 0$ ($\beta = 0.935$, $T = 7$ MeV) clearly corresponds to projectile fragmentation whereas in the $N_h \geqslant$ case we have also the influence of an unknown mechanism.

The angular distributions for the two N_h groups i.e. $1 \leqslant N_h \leqslant 6$ and $N_h > 6$ are given in fig. 3. One observes a slightly broader fragmentation peak for the $1 \leqslant N_h \leqslant 6$ group (fig. 3b), whereas, the tail seems to be larger for the $N_h > 6$ group (fig. 3a); $R_{tp} = 0.29$ for $1 \leqslant N_h \leqslant 6$ events and $R_{tp} = 0.54$ for the $N_h > 6$ sample.
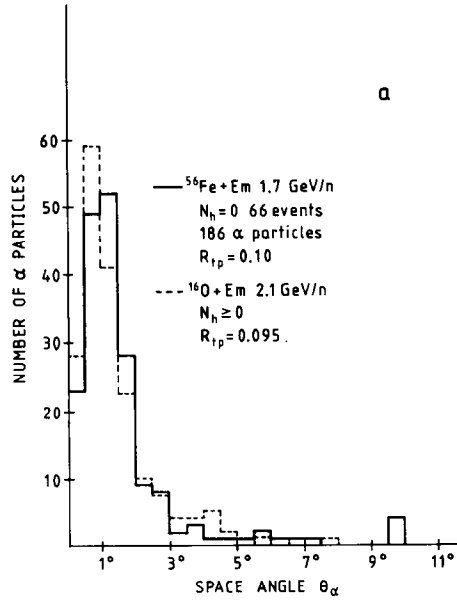
Fig. 1a. Angular distribution for 66 Fe-emulsion reactions with $N_h = 0$; the dotted histogram is the corresponding angular distribution for ^{16}O-emulsion reactions (general sample). Both distributions are normalized to the same number of α-particles.
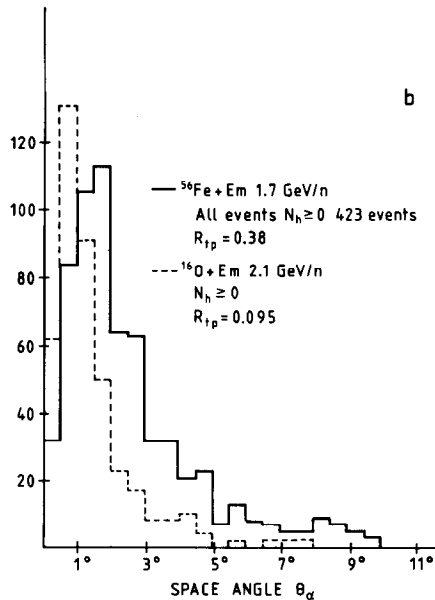
Fig. 1b. Angular distribution for all $(N_h \geqslant 0)$ 423 events; the dotted histogram is the corresponding angular distribution for ^{16}O-emulsion reactions at 2.1 GeV/n. The distributions are normalized to the same number of α-particles in the 0°–2° range.
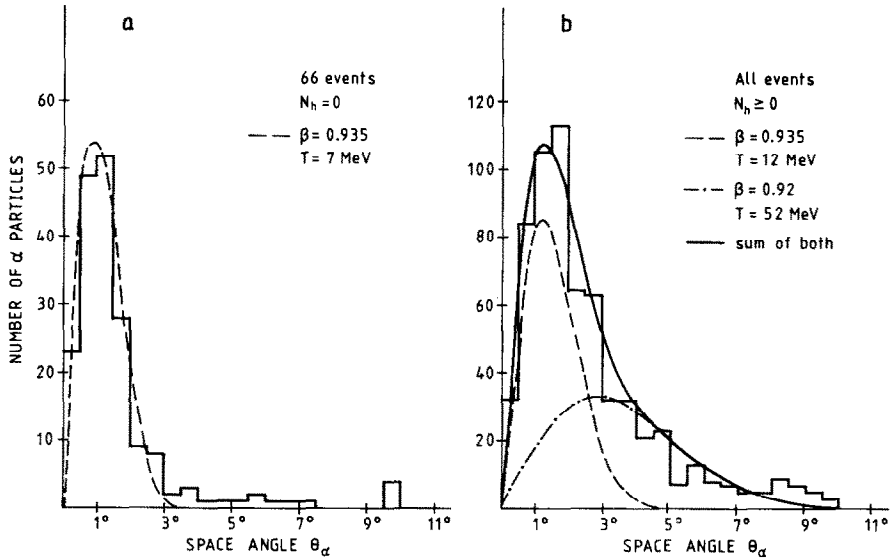
Fig. 2. (a) and (b) are the same angular distributions as given in figs. 1a and 1b. The curves are calculated from moving Boltzmann distributions. In (a) the curve is for $\beta = 0.935$ and $T = 7$ MeV. In (b) the dashed curve is for $\beta = 0.935$ and $T = 12$ MeV; the dot-dashed is for $\beta = 0.92$ and $T = 52$ MeV. The full curve is the sum of these.
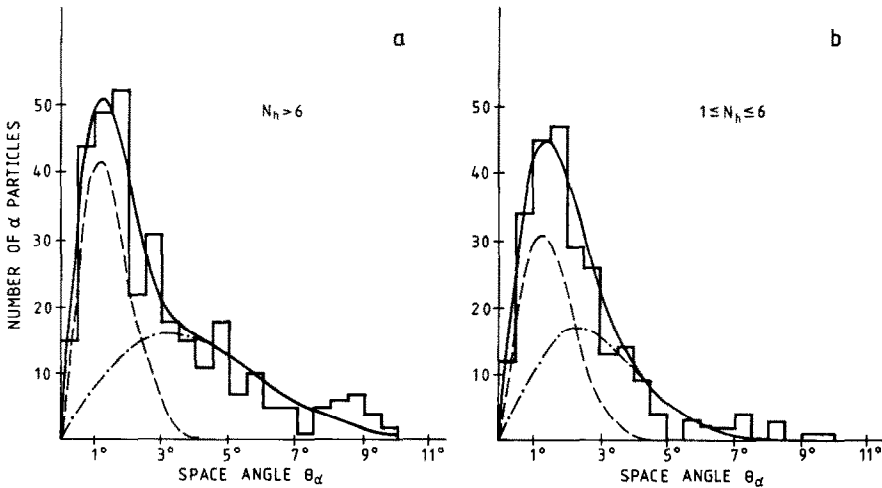
Fig. 3. (a) and (b) are the angular distributions for the $N_h > 6$ and $1 \leq N_h \leq 6$ samples, respectively, (dot-dashed curves are fit to the tail part, dashed to the peak part, and the full curve is the sum of these two). The corresponding values of T_t, β_t, T_p and β_b are given in table 1.
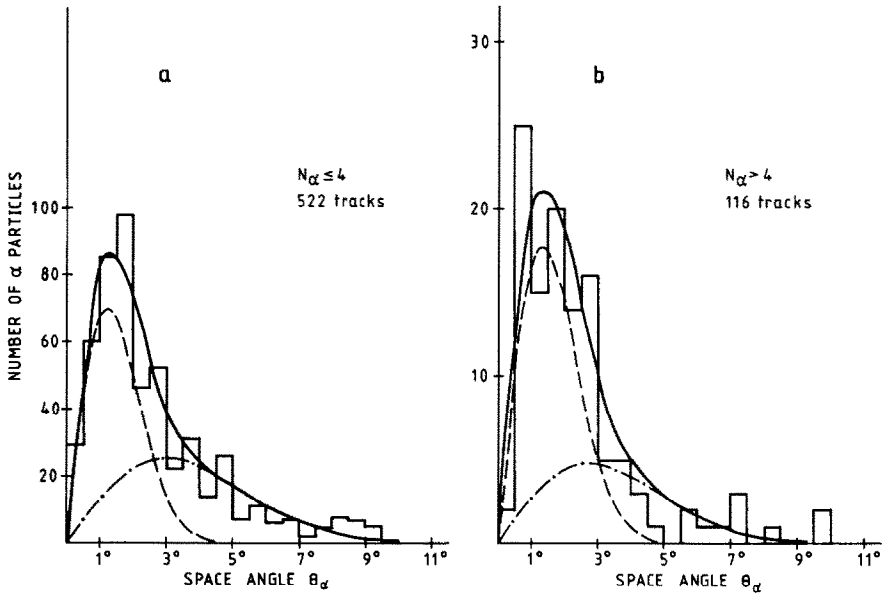
Fig. 4. (a) and (b) are the angular distributions for the $N_\alpha \leqslant 4$ and $N_\alpha > 4$ samples, respectively, (dot-dashed curves are fit to the tail part, dashed to the peak part and the full curve is the sum of these two). The corresponding values of T_t, β_t, T_p and β_p are given in table 1.

The dependence of the angular distribution on the observed α-particle multiplicity (N_α) is illustrated in fig. 4. The fragmentation peak for high N_α events (fig. 4b) is broader than the corresponding peak for low N_α events (fig. 4a). On the other hand the tail for $N_\alpha \leqslant 4$ events is more dominant than the one for $N_\alpha > 4$ events ($R_{tp} = 0.41$ and 0.26, respectively). Large values of θ_α are observed even in reactions with $N_\alpha > 4$.

For comparison the R_{tp} values of all the cases are given in table 1.

3. Comparison with moving Boltzmann distributions

The experimental results show that many α-particles are observed with angles which are larger than the angles expected for α-particles emitted by fragmentation

TABLE 1

Sample	R_{tp}	T_t (MeV)	β_t	T_p (MeV)	β_p
all N_h	0.383 ± 0.029	52	0.92	12	0.935
$N_h = 0$	0.101 ± 0.024			7	0.935
$1 \leqslant N_h \leqslant 6$	0.290 ± 0.039	34	0.92	12	0.935
$N_h > 6$	0.545 ± 0.050	60	0.91	10	0.935
$N_\alpha \leqslant 4$	0.414 ± 0.033	54	0.915	12	0.935
$N_\alpha > 4$	0.261 ± 0.053	48	0.92	14	0.935

from a clean-cut spectator. In an attempt to understand their origin, the experimental distribution is fitted to that originating from a fireball moving with velocity β (in units of c) and heated to a temperature T (MeV). No assumption is made regarding the process of the formation of the fireball or the thermal source. The calculations of the angular distributions of the α-particles emerging from such a thermal source were performed using the following relations [1].

In the rest frame of the source the probability distribution is assumed to be a Boltzmann distribution [5], normalized to unity:

$$\frac{\mathrm{d}^2 p}{p^2 \, \mathrm{d}p \, \mathrm{d}\Omega} = \frac{1}{(4\pi m^3)} \frac{\mathrm{e}^{-E/T}}{\{(T/m)k_0(m/T, 0) + 2(T/m)^2 k_1(m/T, 0)\}},$$

where k_0 and k_1 are complete modified Bessel functions of second order and m, p and E are the mass, 3-momentum and total energy of the α-particle in the source rest frame. The relativistic energy E_L and the magnitude of the 3-momentum P_L in the lab frame are related to E through the Lorentz transformation:

$$E = \gamma(E_L - \beta P_L \cos \theta_L),$$

where θ_L os the polar angle in the lab frame. The following angular distribution [1] can be obtained from probability distribution (2):

$$\frac{\mathrm{d}P}{\mathrm{d}\theta_L} = \frac{\gamma \sin \theta_L}{2I(\alpha)} \left[\frac{4\eta \, \mathrm{e}^{-x}}{(1-\eta^2)^2} \left\{ \frac{1}{x^2} + \frac{1}{x^3} \right\} + \frac{\eta \, \mathrm{e}^{-x}}{(1-\eta^2)} \left\{ \frac{1}{x} + \eta^2 \right\} \right.$$
$$\left. + \frac{(1+\eta^2)}{(1-\eta^2)x} \left\{ k_0(x, t_L) + \frac{2}{x} k_1(x, t_L) \right\} + \frac{\eta^2}{\sqrt{(1-\eta^2)}} k_1(x, t_L) \right]. \qquad (3)$$

Various variables used here are defined as:

$$\alpha = m/T, \qquad x = \gamma\alpha, \qquad \eta = \beta \cos \theta_L,$$

$$x = x\sqrt{1-\eta^2}, \qquad t_L = \ln \sqrt{\frac{1-\eta}{1+\eta}},$$

$$k_0(x, t_L) = \int_{t_L}^{\infty} \mathrm{e}^{-x\cosh U} \, \mathrm{d}U, \ k_1(x, t_L) = x \int_{t_L}^{\infty} \mathrm{e}^{x\cosh U} \sin^2 hU \, \mathrm{d}U,$$

$$I(\alpha) = \frac{2}{\alpha^2} k_1(\alpha, o) + \frac{1}{\alpha} k_0(\alpha, o).$$

(4)

PROCEDURE OF THE ANALYSIS

The calculations of the angular distribution were performed using relation (3) which we call a moving relativistic Boltzmann distribution. In this terminology pure projectile fragmentation will correspond to a fireball with projectile velocity $\beta \sim$ 0.935 and a temperature of 7–8 MeV. This is illustrated in fig. 2a where the peak

for $N_h = 0$ events is well described by a moving relativistic Boltzmann distribution with $\beta = 0.935$ and $T = 7$ MeV.

For comparison we also performed calculations based upon a gaussian momentum distribution in the projectile rest frame [cf. Greiner et al. [4])]. The predictions differ negligibly from the Boltzmann distribution if the width σ_0 of the gaussian distribution is taken to be $\sigma_0^2 = m_\alpha T$. This can be seen if the total relativistic energy $E_\alpha = \sqrt{p_\alpha^2 + m_\alpha^2}$ is expanded as $m_\alpha + P_\alpha^2/2m_\alpha \ldots$, or in other words: since the α particle mass is so large (~ 4 GeV/c^2), it is only for very high momenta that the use of relativistic Boltzmann distributions is essential. For low temperatures, however, high α-momenta are unlikely to occur. Thus we can draw the following conclusions:

(i) The *two* calculated distributions, i.e. the moving relativistic Boltzmann distribution and that given by Greiner et al., are quite similar at this temperature.

(ii) Very few α-particles emitted from pure fragmentation of the projectile have angles greater than 3°. This has prompted us to define R_{tp} as a measure of the non-projectile fragmentation into α-particles.

The further analysis is based upon the second conclusion. The experimental distribution between 3° and 10°, termed as the tail of the angular distribution, is first fitted to moving relativistic Boltzmann distributions with β and T as free parameters. There are many sets of T and β values which give a good fit. The results are given in the β, T plot of fig. 5. Here we can see that if we insist on a velocity β equal to β_{beam} then a large value of the temperature T is required for the moving relativistic Boltzmann distribution. On the other hand the tail can also be fitted to a smaller value of the temperature but then the β-value needed will be appreciably smaller than that of β_{beam}. In the same graph another curve is displayed which gives the 4-momentum conservation constraint assuming that N_p
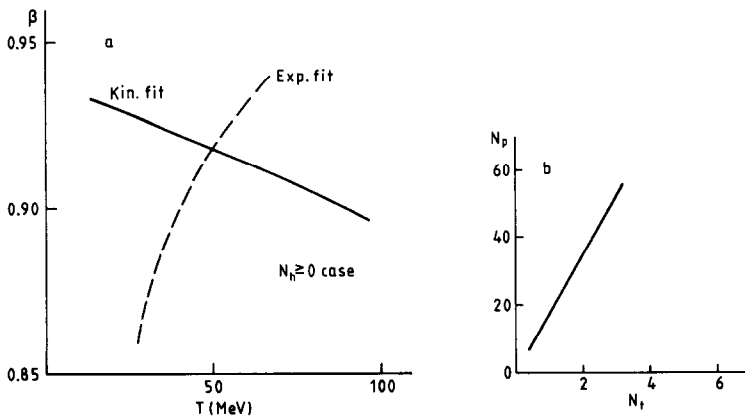
Fig. 5. (a) The full curve is due to kinematically allowed values of β and T whereas the dashed curve is from fitting the experimentally observed angular distribution (fig. 2b) with a moving Boltzmann distribution. (b) shows various N_p, N_t values corresponding to the point of interesection in (a).

and N_t nucleons participate from the projectile and target, respectively, and that all available kinetic energy in the nucleon–nucleon c.m. is completely randomized through elastic collisions. The details of the calculations [5]) are given in the appendix. The intersection of the two curves gives us the kinematically allowed values of β_t and T_t of the thermal source which fit the experimental tail of the angular distribution.

The Boltzmann distribution corresponding to β_t and T_t is extrapolated for angles between 0° and 3°, as shown in fig. 2b. The extrapolated distribution is subtracted from the experimental one. The resulting distribution is thereafter fitted to a moving Boltzmann distribution, assuming the velocity, β_p, to be equal to the velocity of the projectile. The best value of T_p is 10–14 MeV. It would be emphasized here that the peak can also be fitted to a lower temperature (7–8 MeV), but in that case the peak velocity β_p has to be lowered.

A similar analysis has been done for the angular distributions shown in figs. 3 and 4. The resulting values for the best fit of the tail and peak area i.e. T_t, β_t, T_p and β_p are given in table 1.

4. Discussions of other possibilities

(i) One can observe (table 1) that the peak temperature is greater than 7–8 MeV in all the cases except in the $N_h = 0$ sample. This shows that the projectile is heated to a temperature higher than expected from a pure projectile fragmentation process.

(ii) For the tail part, the calculated values of T_t and β_t correspond to a rather peculiar fireball which is kinematically allowed. As shown in fig. 5b the allowed values of N_p/N_t suggest that in such a fireball only a few nucleons from the target participate, which shows that a clean-cut geometrical picture for participants and spectators cannot explain the tail of the angular distribution. A similar conclusion was drawn by Bhalla et al. [6]) in their study of singly charged particles for central reactions of Fe-CNO. A nuclear system could be formed where a major part of the Fe projectile picks up a few (2–3) nucleons from the target followed by thermalization of energy before the α-particles are emitted. Alternatively, a clean-cut fireball may be formed at low velocity and high temperature, which cools by some mechanism (emission of pions, kaons, etc,) before the α-particles are emitted. Both of these explanations seem however to be very unlikely.

Some other possibilities which could produce relativistic α-particles at large angles are discussed below:

(A) α-clusters from the Fe projectile could scatter from individual nucleons (hard scattering) and be observed at large angles, i.e. in the tail area of the angular distributions. In order to explore this possibility Monte Carlo simulations were done by the following procedure.

(i) α-clusters are given random momentum isotropically in the projectile frame, assuming a uniform momentum distribution from zero to some fixed value P_α.

(ii) Similarly, nucleons are given random momentum isotropically in the target frame, assuming a uniform momentum distribution from zero to p_p.

(iii) The collision kinematics are worked out in the c.m. frame of the α and the nucleon and then transformed to the lab frame. For an upper estimate we use S-wave scattering in the common c.m. frame.

The resulting angular distributions for the α-particles do not depend appreciably upon the choice of p_α which is expected because of the large momentum of the projectile itself. But the distributions do depend upon the choice of p_p as shown in fig. 6. One can see that an increase in the momentum p_p only makes the peak (around 14°–15°) broader and the distribution gets flattened.
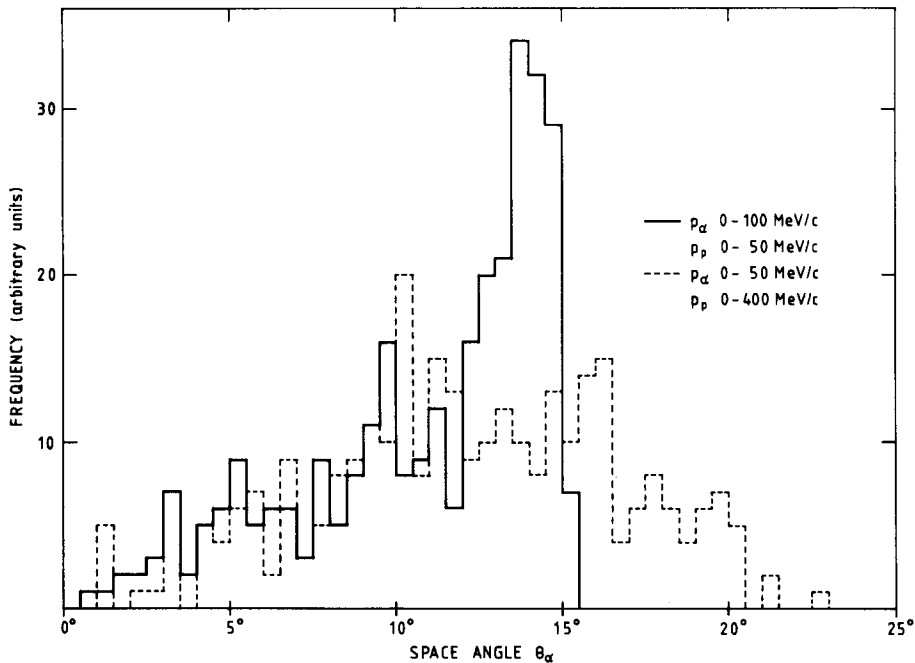
Fig. 6. Two histograms are obtained by Monte Carlo simulations of hard scattering of an α and a nucleon. The full line histogram is for $p_\alpha = 100$ MeV/c and $p_p = 50$ MeV/c, whereas dotted line histogram is for $p_\alpha = 50$ MeV/c and $p_p = 400$ MeV/c.

Based upon these calculations one can say that, qualitatively, α-clusters scattered from nucleons could contribute to the observed relativistic α-particles at large angles. However, as can be seen in fig. 6, the shape of the spectra is not in agreement with the experimental data. As also seen in fig. 6, the shape will also depend upon the exact momentum distribution of the target nucleons which scatter the projectile α-particles.

The exact number of hard α-cluster scattering will depend on the p-α elastic cross section which is fairly large and also on the probability of finding an α-particle

structure in a nucleus. The latter probability will be quite small, except possibly at the nuclear surface, since it means that due to fluctuations in the density 2 protons and 2 neutrons have to come close in space and have relative kinetic energy less than the binding energy of the α-particle. So, although the hard scattering mechanism can contribute some of the α-particles observed at large angles, this process alone can not explain the shape of the whole of the observed tail.

(B) Another possibility could be that the α-particles are produced in a secondary process. In the first step, short-lived fragments of the projectile are produced with large transverse momenta; the relativistic α-particles are subsequently produced by the normal fragmentation of these fragments [7]). These fragments would be produced with transverse momenta large enough to explain the tail part.

There is some indirect evidence which might support such a point of view: firstly, the tail of α-particles is not so pronounced in the $N_h = 0$ sample for the Fe reaction which may originate predominantly from collisions between the Fe nucleus and H or CNO components. Here, collective effects may not be so important, due to the small extensions of the nuclei (cf. also the O-emulsion reactions); secondly, the more pronounced tail for the $N_\alpha \leqslant 4$ sample as compared to $N_\alpha > 4$ events may be due to a larger transverse momentum for the (rather small) fragmenting projectile residue in rather central reactions as compared to peripheral ones (where the projectile residue is large). Since the observed spectra are not selected according to impact parameter, a wide distribution in transverse momentum of the projectile residue (spectator part) will result. Such an effect can clearly explain the tail part of the observed spectra.

The possibility of a radial collective velocity β_r of the α-emitting source can also be discussed [the blast-wave picture of Siemens et al. [8])]. To check if this is feasible let us calculate very roughly the radial velocity of the expanding object necessary to scatter α-particles at 5°–6° in the lab frame. We get: $\tan \theta_L \sim \theta_L \sim P_\perp / P_L = \beta_r / \beta$. Then $\beta_r \approx \beta \frac{5}{180} \pi$ which means that β_r could be at most $\sim 0.1c$. So if the explanation is radial collective flow, very little of the available energy goes into this degree of freedom. However, this possibility cannot be excluded.

5. Conclusions

(I) The comparison of α-particle angular distributions for ^{16}O-emulsion and ^{56}Fe-emulsion reactions at the same energy per nucleon shows that in the Fe case more α-particles are observed at large angles. The angular distributions of a general sample of ^{16}O-emulsion reactions is similar to the $N_h = 0$ sample of Fe-emulsion reactions.

(II) The angular distributions depend upon the N_h values (or target fragmentation) and α-particle multiplicity N_α. The tail part increases with an increased target fragmentation but is reduced with an increase in N_α. Nevertheless there are some α-particles observed at large angles in high N_α events as well as in $N_h = 0$ events.

(III) From the comparison of angular distributions with those calculated using moving relativistic Boltzmann distributions, we conclude the following:

(i) The angular distribution for $N_h = 0$ events can be fitted to a moving Boltzmann distribution with $\beta = \beta_{proj}$ and $T = 7$ MeV; only a few α-particles are outside the calculated distribution. In all other cases the observed angular distribution is fitted to two Boltzmann distributions, one for the tail part and the other for the peak region.

(ii) In order to fit the peak distribution values, temperatures (in events with $N_h > 0$) larger than 7–8 MeV are required for the velocity $\beta = \beta_{proj}$.

(iii) The tail part can be fitted to thermal sources with T_t and β_t values as given in table 1. These kinematically allowed values correspond to a peculiar fireball which cannot be created in a clean-cut participant-spectator picture. One way to make such a fireball is that the Fe-projectile captures a few nucleons from the target, and the energy is thermalized before α-particles are emitted. This is, however, not an easily understandable picture of fireball formation at relativistic energies. It is very unlikely that a fireball can be formed in a clean-cut picture, because it will have too high a temperature and too small a velocity. Such a fireball must be cooled before emitting α-particles.

(IV) Hard scattering of α-particles in the projectile with nucleons from the target could contribute to the tail of the angular distribution at least partially, but the shape of the calculated and observed distributions are qualitatively different.

(V) Collective phenomena might occur, i.e. short-lived heavy fragments might acquire a transverse momentum before they emit the α-particles. Also a radial expansion of a fast moving system might lead to the large scattering of α-particles.

Appendix

The kinematically allowed curve (fig. 5a) is calculated using relativistic kinematics and the assumption that N_p (number of nucleons from the Fe projectile) and N_t (number of nucleons from the target) constitute a fireball. β is calculated from

$$\beta = \frac{P_L}{E_L} = \frac{N_p K (K + 2m')]^{1/2}}{(N_p + N_t)m' + N_p K}.$$

Here we have $K = 1.7$ GeV and m' (the mass of the bound nucleon) is taken to be 0.931 GeV. $E_{c.m.}$ and ε (excitation energy) are calculated from

$$E_{c.m.} = [E_L^2 - p_L^2]^{1/2},$$

$$\varepsilon = \frac{E_{\text{c.m.}}}{N_{\text{p}} + N_{\text{t}}} - m \ .$$

Here m is taken to be 0.938 GeV (mass of the free nucleon). The non-relativistic expression, $\varepsilon = \frac{3}{2}T$, is used to calculate the temperature, assuming further that the fireball is thermalized and that nucleons and α-particles have attained the same temperature. Relativistic calculations do not change the temperature by more than a few percent. It has been found that the kinematically allowed curve depends only on the ratio $N_{\text{p}}/N_{\text{t}}$ rather than on individual values of N_{p} and N_{T}.

References

1) S.I.A. Garpman, Phys. Lett., submitted
2) R.K. Grover *et al.*, in preparation
3) R. Kullberg, private communication
4) D.E. Greiner *et al.*, LBL report 3651 (1975)
5) L.D. Landau and E.M. Lifshitz, Statistical physics (Addison-Wesley, New York, 1969) p. 109; J. Gosset *et al.*, Phys. Rev. **C16** (1977) 1629
6) K.B. Bhalla *et al.*, Phys. Lett. **82B** (1979) 216
7) E.M. Friedlander *et al.*, unpublished
8) P.J. Siemens and J.O. Rasmussen, Phys. Rev. Lett. **42** (1979) 880